A NEW REVERSIBLE DATA HIDING SCHEME EXPLOITING HIGH-DIMENSIONAL PREDICTION-ERROR HISTOGRAM

*Siren Cai, Xiaolong Li, Jiaying Liu and Zongming Guo**

Institute of Computer Science and Technology, Peking University, Beijing 100871, China

ABSTRACT

Pairwise prediction-error expansion (pairwise PEE) is an improvement of the conventional PEE and it can provide excellent performance for reversible data hiding (RDH). Unlike PEE in which the prediction-errors are modified individually, the correlation among prediction-errors is exploited in pairwise PEE by jointly modifying each prediction-error pair. In this paper, the idea of pairwise PEE is developed and a new RDH scheme is proposed. A three-dimensional prediction-error histogram (3D-PEH) is generated by counting every non-overlapped prediction-error triple. Then, data embedding is conducted by modifying the 3D-PEH with a specifically designed reversible mapping. By using 3D-PEH and the proposed reversible mapping, the inter-correlation of prediction-errors is better exploited, and the performance of PEE is significantly enhanced. Moreover, the superiority of our method over pairwise PEE and some other state-of-the-art RDH methods is also experimentally verified. The proposed method is an effective extension of PEE towards the direction of high-dimensional histogram modification.

***Index Terms*—** Reversible data hiding, high-dimensional histogram, prediction-error expansion, histogram modification.

1. INTRODUCTION

Reversible data hiding (RDH) is a specific data hiding technique in which the decoder can extract the exact embedded data and recover the cover medium without any information loss [1, 2]. This technique is currently a hotspot of information hiding and it has been applied to some sensitive applications such as law forensics and medical image processing. Generally, for a desired embedding capacity (EC), the encoder expects to minimize the embedding distortion (measured by PSNR in dB) to obtain a good marked image quality.

In the last decade, many kinds of RDH algorithms have been proposed including the lossless compression based methods [3–5], the difference-expansion (DE) and prediction-error expansion (PEE) based methods [6–21], the histogram-shifting (HS) based methods [22–25] and the integer transformation based methods [26–30], etc. Among those techniques, PEE has attracted considerable attention since it can well exploit the spatial redundancy in natural images. With PEE, a sufficient payload can be embedded into the cover image by modifying the prediction-error histogram (PEH), meanwhile, the embedding distortion can be well controlled by simultaneously utilizing expansion embedding and histogram shifting.

For PEE-based RDH, better exploiting image redundancy usually leads to a superior performance. Based on this idea, most prior PEE methods focus on exploiting inter-pixel correlations to derive accurate prediction in which the prediction-errors are modified individually. However, the correlations among prediction-errors are not considered and utilized in these methods. As mentioned in a recent work [31], the one-dimensional PEH (1D-PEH) employed in PEE, as a low-dimensional projection of image data, is not capable of reflecting the complex dependencies existing among prediction-errors. From this point of view, instead of utilizing prediction-errors individually, a new paradigm of PEE exploiting prediction-error pair is proposed [31, 32]. In these works [31, 32], every two adjacent prediction-errors are counted to generate a two-dimensional PEH (2D-PEH), and a reversible embedding strategy utilizing pairwise PEE or difference-pair mapping (DPM) is adopted for data embedding. The embedding performance of 1D-PEH based RDH is significantly improved by utilizing the new paradigm with 2D-PEH.

In this paper, the idea of pairwise PEE is developed and a new RDH method based on three-dimensional PEH (3D-PEH) is presented. Specifically, a 3D-PEH is first generated by counting every non-overlapped prediction-error triple. Then, data embedding is implemented by modifying the resulting 3D-PEH with a specifically designed reversible mapping. By using 3D-PEH and the proposed reversible mapping, the inter-correlation of prediction-errors is better exploited, and the embedding performance of PEE is significantly enhanced in terms of capacity-distortion evaluation. Moreover, the superiority of our method over pairwise PEE and some other state-of-the-art RDH methods is also experimentally verified. The proposed method is an effective extension of PEE towards the direction of high-dimensional histogram modification.

In the rest of this paper, PEE and pairwise PEE are first briefly reviewed in Section 2. Then, the proposed method and its performance evaluation are introduced in Section 3 and 4, respectively. Finally, we conclude our work in the last section.

2. RELATED WORKS: PEE AND PAIRWISE PEE

The PEE embedding [8–11, 13] contains the following steps. First, according to a certain scanning order, the cover image pixels are collected into a one-dimensional sequence as $(x_1, ..., x_N)$. Then, a predictor is used to determine the prediction of x_i denoted as $\widehat{x}_i$. Next, the prediction-error is computed by $e_i = x_i - \widehat{x}_i$ (suppose here for simplicity that $\widehat{x}_i$ is an integer), and the prediction-error sequence $(e_1, ..., e_N)$ is derived. After that, data embedding is conducted by modifying the prediction-errors, i.e., for a given e_i, it is either expanded or shifted as

$$\widetilde{e}_i = \begin{cases} e_i + m, & \text{if } e_i = 0 \\ e_i - m, & \text{if } e_i = -1 \\ e_i + 1, & \text{if } e_i > 0 \\ e_i - 1, & \text{if } e_i < -1 \end{cases} \tag{1}$$

where $m \in \{0, 1\}$ is a to-be-embedded data bit. Finally, each x_i is modified to $\widetilde{x}_i = \widehat{x}_i + \widetilde{e}_i$ to generate the marked image.

*Corresponding author, e-mail: guozongming@pku.edu.cn

This work is supported by National Natural Science Foundation of China under contract No. 61572052.

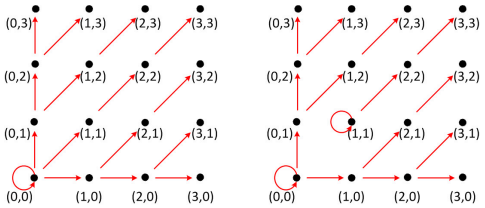

Fig. 1. PEE (left, in the sense of 2D-PEH modification) and pairwise PEE (right).

Consider the 1D-PEH defined as $h_1(a) = |\{i : e_i = a\}|$. Here, $|S|$ means the cardinal number of a set S. The above PEE embedding is actually implemented by modifying the histogram h_1 in which the bins -1 and 0 are expanded to embed data, while the other bins are shifted to create vacancies to ensure the reversibility. Here, an implicit assumption is that -1 and 0 are the two highest bins of h_1.

Recently, instead of modifying prediction-errors individually as (1), a new paradigm of PEE is proposed in [31] by considering the 2D-PEH defined by $h_2(a, b) = |\{i : (e_{2i-1}, e_{2i}) = (a, b)\}|$. In [31], the authors point out that PEE embedding (1) can be implemented equivalently by modifying the 2D-PEH h_2. For example, for a prediction-error pair $(e_{2i-1}, e_{2i}) = (0, 0)$, based on (1), e_{2i-1} will be expanded to 0 or 1 to embed 1 bit, and e_{2i} will also be expanded to 0 or 1 to embed 1 bit. Accordingly, in the case of 2D-PEH modification, the pair $(0, 0)$ will be expanded to one of the four pairs $(0, 0)$, $(0, 1)$, $(1, 0)$ and $(1, 1)$ to embed 2 bits. For another pair $(e_{2i-1}, e_{2i}) = (2, 0)$, in 1D-PEH case, e_{2i-1} will be shifted to 3, and e_{2i} will be expanded to 0 or 1 to embed 1 bit. So, for 2D-PEH, the pair $(2, 0)$ will be expanded to $(3, 0)$ or $(3, 1)$ to embed 1 bit. The equivalent embedding of (1) in the sense of 2D-PEH modification is plotted in the left figure of Fig. 1, in which the modification of prediction-error pairs is illustrated as a mapping of $\mathbb{Z}^2$ using red arrows. That is to say, each pair will be modified as another pair according to the red arrow for data embedding. Particularly, for a given pair (e.g., $(0, 0)$ or $(0, 1)$), the modified pair will be randomly selected if there are more than one arrow starting from it, and in this case, a certain amount of bits (e.g., 2 bits for $(0, 0)$ or 1 bit for $(0, 1)$) will be embedded into it. Here, for the clarity of presentation, only the first quarter of the mapping is plotted.

The paradigm of PEE based on 2D-PEH modification provides a new way for RDH. Based on this approach, the so-called pairwise PEE is proposed by utilizing a new mapping of $\mathbb{Z}^2$ [31]. The idea is to expand or shift bins in a less distorted direction as much as possible. Specifically, for the pair $(0, 0)$ in the left figure of Fig. 1, it is embedded with 2 bits by mapping it to $(0, 0)$, $(0, 1)$, $(1, 0)$ and $(1, 1)$, and the corresponding distortion is 0, 1, 1 and 2, respectively. Clearly, the cost for modifying $(0, 0)$ to $(1, 1)$ is 2, while modifying $(0, 0)$ to $(0, 0)$, $(0, 1)$ or $(1, 0)$ costs much less. So, to reduce the distortion, the modification with high distortion, $(0, 0)$ to $(1, 1)$, is discarded in the mapping. At the same time, the pair $(1, 1)$ can be additionally mapped to itself. In this way, a new mapping is generated as shown in the right figure of Fig. 1. With this new mapping, the pair $(0, 0)$ is embedded with $\log_2 3$ bits instead of 2 bits in PEE, and the pair $(1, 1)$ is embedded with 1 bit while it is just shifted in PEE. Experimental results reported in [31] show that pairwise PEE is better than PEE and the improvement is somewhat significant for low EC cases.

3. PROPOSED METHOD

For pairwise PEE, the basic idea is that adjacent prediction-errors are highly correlated and this type of correlation can be exploited for

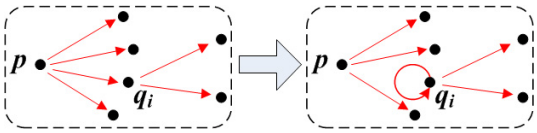

Fig. 2. Excluding q_i from $f_{\mathrm{PEE}}(p)$ to derive a new mapping.

RDH. Clearly, for the prediction-error sequence $(e_1, ..., e_N)$, besides adjacent prediction-errors e_i and e_{i+1}, e_i and e_{i+k} are also correlated for small k since cover pixels are always collected sequentially. Then, enhanced performance can be expected if the inter-correlation of prediction-errors is better utilized. Based on this thought, we propose to design a new RDH based on the modification of the 3D-PEH defined as

$$h_3(a, b, c) = |\{i : (e_{3i-2}, e_{3i-1}, e_{3i}) = (a, b, c)\}|. \tag{2}$$

RDH based on 3D-PEH can be conducted using a mapping $f : \mathbb{Z}^3 \mapsto \mathcal{P}(\mathbb{Z}^3)$ where $\mathcal{P}(\mathbb{Z}^3)$ is the power set of $\mathbb{Z}^3$, i.e., the set composed of all subsets of $\mathbb{Z}^3$. Once $f(p) \neq \emptyset$, and $f(p) \cap f(q) = \emptyset$ holds for every $p, q \in \mathbb{Z}^3$ with $p \neq q$, the reversibility can be guaranteed and such a mapping is called a reversible mapping. Actually, using a reversible mapping, for a cover pixel triple with prediction-errors p, the marked prediction-errors can be taken as an element of $f(p)$, and then the marked pixel triple can be determined accordingly. If $f(p)$ contains more than one element, the marked prediction-errors can be randomly selected as any element of $f(p)$, and in this case, $\log_2 |f(p)|$ bits are embedded into the cover triple. On the other hand, if $|f(p)| = 1$, the cover triple is simply shifted and there is no data embedded into it. In the restoration stage, for a marked triple, we first compute its prediction-errors q, and then recover the original prediction-errors as p which is the unique element of $\mathbb{Z}^3$ satisfying $q \in f(p)$. Simultaneously, the embedded data can be extracted if $|f(p)| > 1$. By this approach, the EC is $\sum_{p\in\mathbb{Z}^3} h_3(p) \log_2 |f(p)|$, and the embedding distortion (the mean-squared error) can be estimated as

$$\sum_{p\in\mathbb{Z}^3} h_3(p) \left(\sum_{q\in f(p)} \frac{\|q - p\|_{l^2}^2}{|f(p)|} \right) \tag{3}$$

where $\|\cdot\|_{l^2}$ is the l^2-norm.

Notice that, like the case of pairwise PEE, the PEE embedding (1) can be implemented equivalently by modifying the 3D-PEH h_3 as well. Specifically, we can take a reversible mapping $f : \mathbb{Z}^3 \mapsto \mathcal{P}(\mathbb{Z}^3)$ as, for each $(a_1, a_2, a_3) \in \mathbb{Z}^3$

$$f(a_1, a_2, a_3) = \{(b_1, b_2, b_3) : b_i \in g(a_i), i \in \{1, 2, 3\}\} \tag{4}$$

where $g : \mathbb{Z} \mapsto \mathcal{P}(\mathbb{Z})$ is a function defined by $g(0) = \{0, 1\}$, $g(-1) = \{-1, -2\}$, $g(x) = \{x+1\}$ if $x > 0$, and $g(x) = \{x-1\}$ if $x < -1$. For example, $f(0, 1, -2) = \{(0, 2, -3), (1, 2, -3)\}$. Then, according to the aforementioned embedding procedure based on the reversible mapping (4), one can verify that the resulting RDH is just the PEE embedding (1). For the sake of clarity, the reversible mapping f in (4) is denoted as f_{PEE} in the following context.

We will iteratively adjust f_{PEE} to derive a new reversible mapping denoted as f_{PRO}. Then, the proposed method is implemented based on 3D-PEH modification using f_{PRO}. Specifically, for $p \in \mathbb{Z}^3$ with $f_{\mathrm{PEE}}(p) = \{q_1, ..., q_n\}$ and $n > 1$, some q_i with large embedding cost $\|p - q_i\|_{l^2}$ will be excluded from the set $f_{\mathrm{PEE}}(p)$. At the same time, for each excluded q_i, it will be added to the set $f_{\mathrm{PEE}}(q_i)$. For example, if there is only one $(p, q_i) \in \mathbb{Z}^3 \times \mathbb{Z}^3$ such that q_i is excluded from $f_{\mathrm{PEE}}(p)$, the adjusted mapping f is

$$f(q) = \begin{cases} f_{\mathrm{PEE}}(q) - \{q_i\}, & \text{if } q = p \\ f_{\mathrm{PEE}}(q) \cup \{q_i\}, & \text{if } q = q_i \\ f_{\mathrm{PEE}}(q), & \text{otherwise} \end{cases}. \tag{5}$$

The adjustment process (5) based on one pair $(p, q_i) \in \mathbb{Z}^3 \times \mathbb{Z}^3$ exclusion-adding (OPEA) operation to derive a new reversible mapping is illustrated in Fig. 2.

Notice that, according to (4), for every $(a_1, a_2, a_3) \in \mathbb{Z}^3$, we have the following symmetric property

$$f_{\text{PEE}}(\pi_1(a_1), \pi_2(a_2), \pi_3(a_3)) = \{(\pi_1(b_1), \pi_2(b_2), \pi_3(b_3)) : b_i \in g(a_i), i \in \{1, 2, 3\}\} \quad (6)$$

where $\pi_i(x) = x$ or $\pi_i(x) = -1 - x$, for each $i \in \{1, 2, 3\}$. Then, we define $f_{\text{PRO}}(p)$ only for $p \in \mathbb{Z}^3_+ = \{(a_1, a_2, a_3) : a_i \geq 0, i \in \{1, 2, 3\}\}$. The other triples of $\mathbb{Z}^3$ can be defined by imposing the same symmetric property (6) to f_{PRO}.

We now introduce how to select the to-be-excluded triples for OPEA. Once a set of to-be-excluded triples is selected, f_{PRO} can be defined by using OPEA iteratively. Notice that, according to (4), for $(a_1, a_2, a_3) \in \mathbb{Z}^3_+$, it will be embedded with data if and only if at least one a_i is 0. Then, motivated by pairwise PEE, the following triples (b_1, b_2, b_3) introducing large embedding cost are selected:

- $(b_1, b_2, b_3) \in f_{\text{PEE}}(0, 0, 0)$ with $b_1 + b_2 + b_3 > 1$,
- for each $a \geq 1$, $(b_1, b_2, b_3) \in f_{\text{PEE}}(a, 0, 0)$ with $b_2 + b_3 > 1$,
- for each $a \geq 1$, $(b_1, b_2, b_3) \in f_{\text{PEE}}(0, a, 0)$ with $b_1 + b_3 > 1$,
- for each $a \geq 1$, $(b_1, b_2, b_3) \in f_{\text{PEE}}(0, 0, a)$ with $b_1 + b_2 > 1$.

That is, the to-be-excluded triple set contains following elements:

- $(0, 1, 1)$, $(1, 0, 1)$, $(1, 1, 0)$, $(1, 1, 1)$,
- $(a + 1, 1, 1)$, $(1, a + 1, 1)$ and $(1, 1, a + 1)$, for $a \geq 1$.

More specifically, four triples $(0, 1, 1)$, $(1, 0, 1)$, $(1, 1, 0)$ and $(1, 1, 1)$ are excluded from $f_{\text{PEE}}(0, 0, 0)$, i.e., we have

$$f_{\text{PRO}}(0, 0, 0) = \{(0, 0, 0), (1, 0, 0), (0, 1, 0), (0, 0, 1)\}. \quad (7)$$

By this definition, instead of embedding 3 bits into $(0, 0, 0)$ in PEE, only 2 bits is embedded into $(0, 0, 0)$ in our method while the average embedding distortion for this triple is reduced from $(0 + 1 \times 3 + 2 \times 3 + 3)/8 = 1.5$ to $(0 + 1 \times 3)/4 = 0.75$. Accordingly, by applying the "adding" operation to the excluded triples, we have

$$\begin{cases} f_{\text{PRO}}(0, 1, 1) = \{(0, 1, 1), (0, 2, 2), (1, 2, 2)\} \\ f_{\text{PRO}}(1, 0, 1) = \{(1, 0, 1), (2, 0, 2), (2, 1, 2)\} \\ f_{\text{PRO}}(1, 1, 0) = \{(1, 1, 0), (2, 2, 0), (2, 2, 1)\} \\ f_{\text{PRO}}(1, 1, 1) = \{(1, 1, 1), (2, 2, 2)\} \end{cases}. \quad (8)$$

For these four triples, the embedding distortion is also reduced while the amount of embedded data bits is increased.

On the other hand, for the triple $(a, 0, 0)$ with $a \geq 1$, we have

$$f_{\text{PRO}}(a, 0, 0) = \{(a + 1, 0, 0), (a + 1, 0, 1), (a + 1, 1, 0)\}. \quad (9)$$

That is, instead of embedding 2 bits into $(a, 0, 0)$ in PEE, $\log_2 3$ bits is embedded into $(a, 0, 0)$ in our method. And, the average embedding distortion for this triple is reduced from $(1 + 2 \times 2 + 3)/4 = 2$ to $(1 + 2 \times 2)/3 = 5/3$. Accordingly, we have

$$f_{\text{PRO}}(a + 1, 1, 1) = \{(a + 1, 1, 1), (a + 2, 2, 2)\}. \quad (10)$$

Then, 1 bit is embedded into $(a + 1, 1, 1)$ in our method while it is just shifted in PEE, and the embedding distortion for this triple is reduced as well.

With f_{PRO}, one can verify that the embedding distortion of the resulting RDH is reduced compared with that of f_{PEE}. Moreover, the EC is enlarged if the following inequality holds,

$$\sum_{p \in E_A} h_3(p) + (\theta - 1) \sum_{p \in E_B} h_3(p) > \sum_{p \in E_C} h_3(p) + (2 - \theta) \sum_{p \in E_D} h_3(p) \quad (11)$$

where $\theta = \log_2 3$, A, B, C, D are four sets defined by

- $A = \{(1, 1, 1)\} \cup \{(b, 1, 1), (1, b, 1), (1, 1, b) : b > 1\}$
- $B = \{(0, 1, 1), (1, 0, 1), (1, 1, 0)\}$
- $C = \{(0, 0, 0)\}$
- $D = \{(a, 0, 0), (0, a, 0), (0, 0, a) : a \geq 1\}$

and for each $S \in \{A, B, C, D\}$, E_S is the expanded set of S considering the symmetric property implied in (6), i.e., E_S is the set $\{(b_1, b_2, b_3) : (a_1, a_2, a_3) \in S, b_i \in \{a_i, -1 - a_i\}, i \in \{1, 2, 3\}\}$, e.g., $E_C = \{(b_1, b_2, b_3) : b_i \in \{0, -1\}\}$.

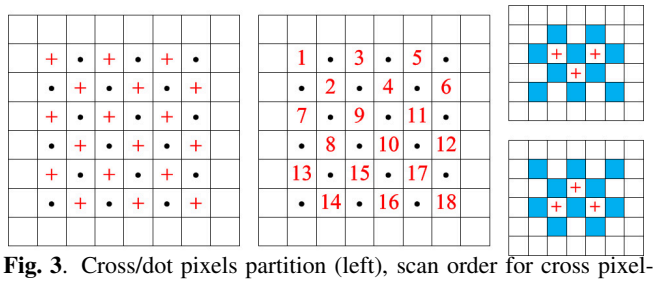

Fig. 3. Cross/dot pixels partition (left), scan order for cross pixels (center), and the context (blue pixels) for complex measurement computation for a cross pixel triple (right).

Based on (11), theoretical analysis can be conducted for the performance comparison between the proposed method and PEE. Actually, the inequality (11) is generally true for the common test images. As a result, with less distortion and enlarged EC, the proposed method based on 3D-PEH and f_{PRO} generally provides a better embedding result than PEE.

Our data embedding procedure is briefly described as follows. The same as [10], rhombus prediction and double-layered embedding are adopted in our implementation. For double-layered embedding, the cover image is divided into two sets denoted as "cross" and "dot" (see the left figure of Fig. 3), and then successively, the cross and dot sets are embedded with half of the secret message, respectively. Since the two layers' embedding are processed similarly, we only take the cross layer for illustration.

Referring to the center figure of Fig. 3, except for pixels located in borders, the cross pixels are scanned from left to right and top to bottom to derive the cover sequence $(x_1, ..., x_N)$. Here, to avoid the overflow and underflow, the pixels valued 0 will be changed to 1, and the pixels valued 255 will be changed to 254. Meanwhile, a location map will be established to record these problematic locations. The location map is a binary sequence sized N and it will be losslessly compressed to reduce its size. The compressed location map will be embedded into the cover image along with the secret message for blind extraction. Then, each x_i is predicted using its four dot neighbors as the inter-valued average to determine $\widehat{x}_i$ and $e_i = x_i - \widehat{x}_i$. Lastly, data embedding is conducted by modifying prediction-errors $(e_1, ..., e_N)$ based on the 3D-PEH h_3 and the proposed reversible mapping f_{PRO}.

To further enhance the embedding performance, we apply the pixel-selection (PS) strategy [31, 33] to our method. That is, for each pixel triple (see the right figure of Fig. 3 for an illustration of cross pixels), its complexity measurement is computed as the sum of every two connected pixels (in both diagonal and anti-diagonal directions) in its context containing 10 pixels. Then, for a given threshold T, only the triples with complexity less than T will be utilized for data embedding while others are ignored. In our implementation, the threshold T is iteratively determined as the smallest positive integer such that the payload can be embedded.

Finally, we remark that, our data extraction and cover image recovery procedure is just the inverse of data embedding. In a reverse pixel scan order, we first extract the half capacity and realize restoration for dot pixels. Then, we extract the rest half capacity and realize restoration for cross pixels. The routine description for data extraction and image recovery is omitted here due to space limitation.

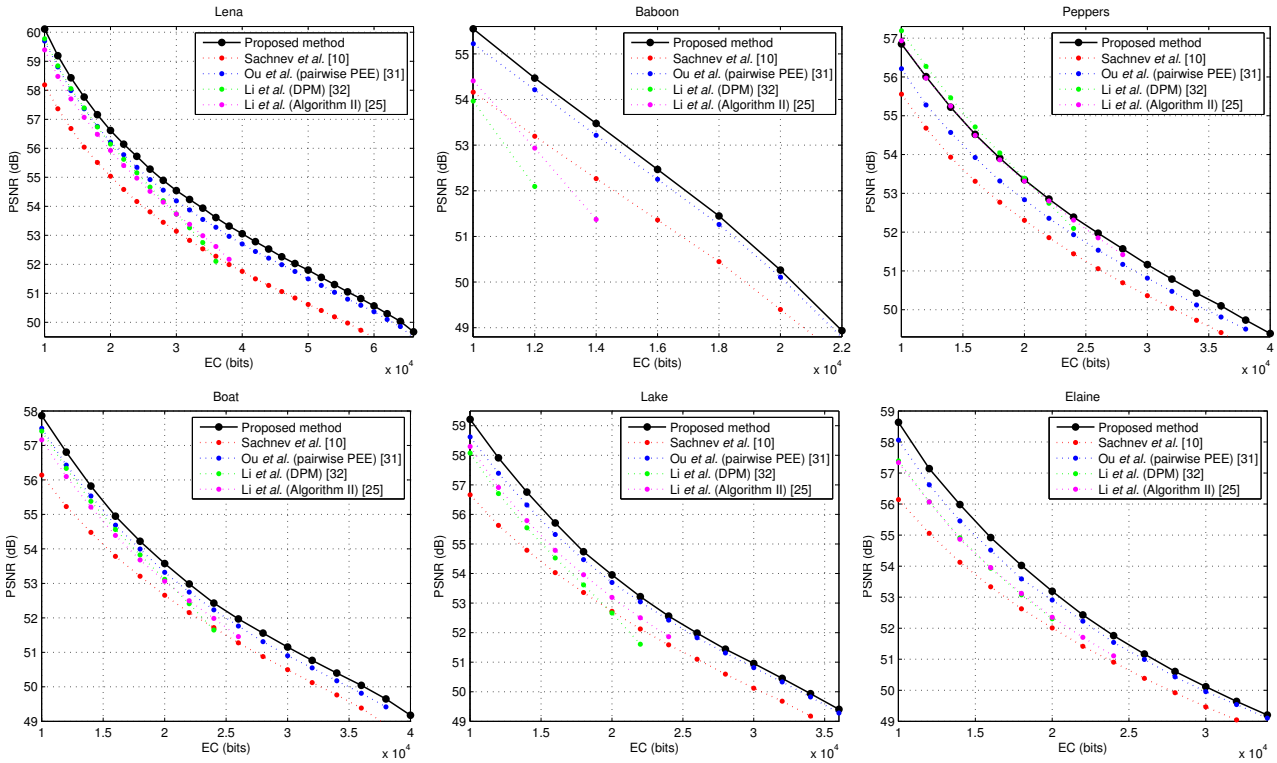

Fig. 4. Performance comparison between our method and the methods of Sachnev *et al.* [10], Ou *et al.* [31], Li *et al.* [32] and Li *et al.* [25].

Table 1. Comparison of PSNR (in dB) between the proposed method and the methods of Sachnev *et al.* [10], Ou *et al.* [31], Li *et al.* [32] and Li *et al.* (Algorithm II) [25], for a capacity of 10,000 bits.

Image	[10]	[31]	[32]	[25]	Proposed
Lena	58.19	59.75	59.78	59.37	60.12
Baboon	54.16	55.21	53.96	54.41	55.55
Peppers	55.55	56.21	57.19	56.89	56.85
Boat	56.15	57.55	57.42	57.16	57.87
Lake	56.66	58.72	58.08	58.27	59.22
Elaine	56.14	58.06	57.39	57.34	58.64
Average	**56.14**	**57.58**	**57.30**	**57.24**	**58.04**

4. EXPERIMENTAL RESULTS

The proposed method is evaluated by comparing it with the conventional PEE [10], pairwise PEE [31], DPM-based RDH [32] and Algorithm II of [25]. The comparison is conducted on six 512×512 sized gray-scale images including Lena, Baboon, Peppers, Boat, Lake and Elaine. All these images are downloaded from USC-SIPI database (http://sipi.usc.edu/database/database.php?volume=misc). The performance comparison is shown in Fig. 4 in which EC varies from 10,000 bits to the maximum capacity of the proposed method with a step of 2,000 bits.

For PEE embedding [10], the prediction and double-layered embedding employed in this method are the same as ours. In addition, a PS technique based on local variance sorting is used in this method as well. It is a well-performed and representative RDH algorithm. However, according to Fig. 4, our method significantly outperforms [10] with a larger PSNR whatever test image or EC is. Referring to Table 1, our method outperforms [10] with an average increase of PSNR by 1.9 dB for an EC of 10,000 bits.

Pairwise PEE [31] and the method [32] are based on 2D-PEH modification. For pairwise PEE, the 2D-PEH is generated by counting adjacent prediction-errors. For [32], the 2D-PEH is generated by considering each pixel pair and its context to derive a difference pair. Then, data embedding is implemented by modifying the resulting 2D-PEH with a specific reversible mapping (for [32], the reversible mapping is called DPM). These 2D-PEH based methods perform better than the ones based on 1D-PEH, e.g., [10, 13]. However, the experimental results show that our method is better than [31] and [32] in most cases. According to Table 1, for an EC of 10,000 bits, our method outperforms [31] and [32] with an average increase of PSNR by 0.46 and 0.74 dB, respectively. We believe that our advantage mainly lies in high-dimensional PEH utilization.

The Algorithm II proposed in [25] is also based on histogram modification by utilizing a specific prediction strategy. It performs well for low EC with a superior performance compared with some state-of-the-art works [9, 13, 33, 34]. However, according to Table 1, our method outperforms this method with an average increase of PSNR by 0.8 dB for an EC of 10,000 bits.

5. CONCLUSION

This work is an extension of PEE based on 3D-PEH modification. The proposed data embedding is conducted by modifying 3D-PEH with an advisable reversible mapping. Our superiority over PEE [10], pairwise PEE [31] and some other state-of-the-art works [25, 32] is experimentally verified, demonstrating the effectiveness of the high-dimensional histogram utilization in RDH.

In the future, instead of 3D-PEH, we will extend the proposed method to larger prediction-error group consisting more prediction-errors. Moreover, other than the proposed one, we will try to design effective reversible mappings especially the content-adaptive ones for high-dimensional histogram based RDH. Incorporating the proposed embedding method with more advanced histogram generation methods such as [35, 36] is also one of our future work.

References

[1] Y. Q. Shi, "Reversible data hiding," in *Proc. IWDW*, 2004.

[2] Y. Q. Shi, Z. Ni, D. Zou, C. Liang, and G. Xuan, "Lossless data hiding: fundamentals, algorithms and applications," in *Proc. IEEE ISCAS*, 2004.

[3] J. Fridrich, M. Goljan, and R. Du, "Lossless data embedding - New paradigm in digital watermarking," *EURASIP J. Appl. Signal Process.*, vol. 2002, no. 2, pp. 185–196, 2002.

[4] M. U. Celik, G. Sharma, A. M. Tekalp, and E. Saber, "Lossless generalized-LSB data embedding," *IEEE Trans. Image Process.*, vol. 14, no. 2, pp. 253–266, 2005.

[5] M. U. Celik, G. Sharma, and A. M. Tekalp, "Lossless watermarking for image authentication: A new framework and an implementation," *IEEE Trans. Image Process.*, vol. 15, no. 4, pp. 1042–1049, 2006.

[6] J. Tian, "Reversible data embedding using a difference expansion," *IEEE Trans. Circuits Syst. Video Technol.*, vol. 13, no. 8, pp. 890–896, 2003.

[7] L. Kamstra and H. J. A. M. Heijmans, "Reversible data embedding into images using wavelet techniques and sorting," *IEEE Trans. Image Process.*, vol. 14, no. 12, pp. 2082–2090, 2005.

[8] D. Thodi and J. Rodriguez, "Expansion embedding techniques for reversible watermarking," *IEEE Trans. Image Process.*, vol. 16, no. 3, pp. 721–730, 2007.

[9] Y. Hu, H. Lee, and J. Li, "DE-based reversible data hiding with improved overflow location map," *IEEE Trans. Circuits Syst. Video Technol.*, vol. 19, no. 2, pp. 250–260, 2009.

[10] V. Sachnev, H. J. Kim, J. Nam, S. Suresh, and Y. Q. Shi, "Reversible watermarking algorithm using sorting and prediction," *IEEE Trans. Circuits Syst. Video Technol.*, vol. 19, no. 7, pp. 989–999, 2009.

[11] W. Hong, T. Chen, and C. Shiu, "Reversible data hiding for high quality images using modification of prediction errors," *Journal of Systems and Software*, vol. 82, no. 11, pp. 1833–1842, 2009.

[12] W. L. Tai, C. M. Yeh, and C. C. Chang, "Reversible data hiding based on histogram modification of pixel differences," *IEEE Trans. Circuits Syst. Video Technol.*, vol. 19, no. 6, pp. 906–910, 2009.

[13] L. Luo, Z. Chen, M. Chen, X. Zeng, and Z. Xiong, "Reversible image watermarking using interpolation technique," *IEEE Trans. Inf. Forens. Security*, vol. 5, no. 1, pp. 187–193, 2010.

[14] D. Coltuc, "Improved embedding for prediction-based reversible watermarking," *IEEE Trans. Inf. Forens. Security*, vol. 6, no. 3, pp. 873–882, 2011.

[15] G. Coatrieux, W. Pan, N. Cuppens-Boulahia, F. Cuppens, and C. Roux, "Reversible watermarking based on invariant image classification and dynamical error histogram shifting," *IEEE Trans. Inf. Forens. Security*, vol. 8, no. 1, pp. 111–120, 2013.

[16] C. Qin, C.-C. Chang, Y.-H. Huang, and L.-T. Liao, "An inpainting-assisted reversible steganographic scheme using a histogram shifting mechanism," *IEEE Trans. Circuits Syst. Video Technol.*, vol. 23, no. 7, pp. 1109–1118, 2013.

[17] W. Zhang, X. Hu, X. Li, and N. Yu, "Recursive histogram modification: establishing equivalency between reversible data hiding and lossless data compression," *IEEE Trans. Image Process.*, vol. 22, no. 7, pp. 2775–2785, 2013.

[18] X. Zhang, "Reversible data hiding with optimal value transfer," *IEEE Trans. multimedia*, vol. 15, no. 2, pp. 316–325, 2013.

[19] L. Dong, J. Zhou, Y. Tang, and X. Liu, "Estimation of capacity parameters for dynamic histogram shifting (DHS)-based reversible image watermarking," in *Proc. IEEE ICME*, 2014.

[20] I. Dragoi and D. Coltuc, "Local-prediction-based difference expansion reversible watermarking," *IEEE Trans. Image Process.*, vol. 23, no. 4, pp. 1779–1790, 2014.

[21] I. Dragoi and D. Coltuc, "On local prediction based reversible watermarking," *IEEE Trans. Image Process.*, vol. 24, no. 4, pp. 1244–1246, 2015.

[22] Z. Ni, Y. Shi, N. Ansari, and W. Su, "Reversible data hiding," *IEEE Trans. Circuits Syst. Video Technol.*, vol. 16, no. 3, pp. 354–362, 2006.

[23] S. K. Lee, Y. H. Suh, and Y. S. Ho, "Reversible image authentication based on watermarking," in *Proc. IEEE ICME*, 2006.

[24] M. Fallahpour, "Reversible image data hiding based on gradient adjusted prediction," *IEICE Electronics Express*, vol. 5, no. 20, pp. 870–876, 2008.

[25] X. Li, B. Li, B. Yang, and T. Zeng, "General framework to histogram-shifting-based reversible data hiding," *IEEE Trans. Image Process.*, vol. 22, no. 6, pp. 2181–2191, 2013.

[26] D. Coltuc and J. Chassery, "Very fast watermarking by reversible contrast mapping," *IEEE Signal Process. Lett.*, vol. 14, no. 4, pp. 255–258, 2007.

[27] S. Weng, Y. Zhao, J. Pan, and R. Ni, "Reversible watermarking based on invariability and adjustment on pixel pairs," *IEEE Signal Process. Lett.*, vol. 15, pp. 721–724, 2008.

[28] X. Wang, X. Li, B. Yang, and Z. Guo, "Efficient generalized integer transform for reversible watermarking," *IEEE Signal Process. Lett.*, vol. 17, no. 6, pp. 567–570, 2010.

[29] D. Coltuc, "Low distortion transform for reversible watermarking," *IEEE Trans. Image Process.*, vol. 21, no. 1, pp. 412–417, 2012.

[30] F. Peng, X. Li, and B. Yang, "Adaptive reversible data hiding scheme based on integer transform," *Signal Processing*, vol. 92, no. 1, pp. 54–62, 2012.

[31] B. Ou, X. Li, Y. Zhao, R. Ni, and Y. Q. Shi, "Pairwise prediction-error expansion for efficient reversible data hiding," *IEEE Trans. Image Process.*, vol. 22, no. 12, pp. 5010–5021, 2013.

[32] X. Li, W. Zhang, X. Gui, and B. Yang, "A novel reversible data hiding scheme based on two-dimensional difference-histogram modification," *IEEE Trans. Inf. Forens. Security*, vol. 8, no. 7, pp. 1091–1100, 2013.

[33] X. Li, B. Yang, and T. Zeng, "Efficient reversible watermarking based on adaptive prediction-error expansion and pixel selection," *IEEE Trans. Image Process.*, vol. 20, no. 12, pp. 3524–3533, 2011.

[34] W. Hong, "Adaptive reversible data hiding method based on error energy control and histogram shifting," *Optics Communications*, vol. 285, no. 2, pp. 101–108, 2012.

[35] I.-C. Dragoi, D. Coltuc, and I. Caciula, "Horizontal pairwise reversible watermarking," in *Proc. EUSIPCO*, 2015.

[36] X. Li, W. Zhang, X. Gui, and B. Yang, "Efficient reversible data hiding based on multiple histograms modification," *IEEE Trans. Inf. Forens. Security*, vol. 10, no. 9, pp. 2016–2027, 2015.